Mechano-modulation of Burn Wound Repair

Honors Research Thesis

Presented in partial fulfillment of the requirements for graduation
with honors research distinction in the undergraduate colleges of The Ohio State University

by

James Willard

The Ohio State University
June 2012

Project Advisor: Dr. Heather Powell
Materials Science and Engineering
Biomedical Engineering

Abstract

Scarring is a common complication following second degree or deeper burn wounds. Compressive forces, produced by pressure garments, have been shown to prevent excessive contracture and scarring following burn wounds. Despite this evidence, little is known regarding the optimal magnitude or duration of force or the molecular mechanisms responsible for these benefits. The purpose of this study was to uncover the mechanisms by which compression therapy functions and develop new mechanically-based therapies to prevent post-burn scarring while maintaining high patient compliance. Full-thickness burn wounds were generated on Red Duroc pigs using an electronic microstat-controlled heat delivery device which was heated to 200 + 5 ºC and placed on the porcine skin for 30 seconds. Wounds were allowed to heal for 28 days after which 10% compression was applied to half the wounds via F47 compression fabric. Wound area, wound perfusion, and wound hardness and elasticity were quantified at days 0, 28, 42, 56, 78 using computerized planimetry, Laser Doppler and torsional ballistometry, respectively. Wound morphology was assessed at days 28, 56 and 78 using histology, immunohistochemistry and transmission electron microscopy. The use of compression reduced wound contraction with control skin contracting to 65 ± 5.31% original area at day 78 and wounds receiving compression contracting to 85 ± 5.70% original area. Compression therapy slightly reduced skin hardness, helped to return skin elasticity, and increased ultimate tensile strength and linear stiffness of skin. Wound perfusion and collagen fibril deposition were not found to cause the observed differences, but future studies will investigate the role inflammation and molecular pathways play in this process.

Acknowledgements

I would like to express my deepest gratitude for Dr. Heather Powell, whose continuous guidance and support throughout the past two years have shaped me as a student, scientist and person. She has given me opportunities that I would not have had otherwise, and has served as an inspiration to me and my laboratory peers. My undergraduate career at The Ohio State University was greatly enriched as a result of having her as my mentor, and I will always reflect upon my experience in her laboratory with fond memories and great appreciation.

I would also like to thank Drs. Roy, Gardillo, and Sen, in addition to Dr. Haytham Elgharably and Mr. Jason Driggs for their assistance and support throughout the duration of this study. Also, the ULAR staff and resources were instrumental in the success of this project. Thank you to Anna, Kuazee Mona, Gïrta, Miss Piggy, No Name, and Oinkers for being selfless bundles of joy during the 78 days that I knew you.

I would also like to thank the Arts and Sciences Honors Office for their Undergraduate Research Scholarship that was used to provide financial support while I was conducting this research. My undergraduate experience at this university has been life-changing as a result.

Table of Contents

Chapters

List of Figures

Chapter 1

Introduction

Scarring is a common complication following second degree or deeper burn wounds. Without medical treatment, burn wounds form nonpliable, weak scar tissue which can cause pain, inflammation, and itching and significantly reduce range of mobility[1,2]. The current state of the art in mechano-modulation of scar formation following a burn injury is the use of compression garments which create a static pressure on the skin[3-8]. While the clinical efficacy of compression therapy has not been proven, there is a large amount of research that suggests compression garments prevent excessive contracture and scarring, and improve skin elasticity and range of motion following burn wounds[9-15].

It is believed that the pressure exerted by the garments causes decreased blood, oxygen and nutrient supplies to the wounds and results in lower levels of collagen production[6,13,16-18]. Despite this evidence, little is known regarding the optimal magnitude, duration of force, or the molecular mechanisms responsible for these benefits. Higher magnitudes of pressure (>25 mm Hg) have been associated with rapid results[13,19] while similar pressures have also caused scar breakdown and ulceration[13,20].

Compression garments are tight, itchy and uncomfortable and have an unflattering appearance (Fig. 1.1). Patients are required to wear these garments for at least 23 hours per day for up to 2-3 years. Garment stiffness, discomfort from heat and perspiration and poor aesthetic properties of the garments lead to high levels of non-compliance, with only 41% of patients reported as being fully compliant[21,22]. Although patient compliance is

low due to the discomfort and social stigma associated with wearing these garments, no significant advances to this therapy have been developed over the past 35 years[21-24].

The purpose of this study was to uncover the mechanisms by which compression therapy functions and develop new mechanically-based therapies to prevent post-burn scarring while maintaining high patient compliance. The short term goal is to develop novel mechanically based therapies that can reduce the required pressure applications to one or two per day and increase patient compliance. If the molecular mechanisms behind the response to compression therapy are discovered, a long term goal would be to develop non-mechanically based solutions that up or down regulate these pathways.

Compressive forces generated by compression garments

Fig 1.1 Full body compression garment. Patients are required to wear these garments for at least 23 hours per day, up to 2-3 years. They are unflattering as well as uncomfortable, resulting in very low patient compliance.

Chapter 2

Experimental Design

In order to obtain clinically relevant results, a porcine animal model was used. Many factors are important when choosing an animal model for research. Since this study was focused on developing new therapies to improve burn wound healing in humans, scientific relevance was most important. In regards to the biology of wound healing, small mammals differ from humans both anatomically and physiologically. Some differences are that small mammals have a dense layer of body hair and a thin dermis and epidermis. Additionally, they heal primarily through wound contraction as opposed to the re-epithelialization process that humans display. Compared to other small animals, porcine skin is a closer anatomical and physiological match to human skin. Prior studies investigating wound healing in pigs show a 78% concordance with human wound healing[25].

To investigate the effect compression has on wound repair, aspects of skin biomechanics and the cellular responses behind such observations were investigated throughout the 78 day study (Fig. 2.1). Biomechanically, skin hardness and elasticity, as well as ultimate tensile strength and linear stiffness, are important indicators of skin quality and viability. To explain these measurements molecularly, blood and oxygen flow, collagen deposition, inflammation and molecular pathways affecting collagen synthesis were investigated. This study sought to elucidate the role compressive force plays in scar tissue modulation by investigating these areas in particular.

To inflict burn wounds on the porcine, a novel burn device was developed which heated the skin to 100 °C for thirty seconds and generated full thickness burn wounds.

After allowing the wounds to dry and re-epithelialize, compression garments were wrapped around half the wounds. Wound area was calculated using computerized planimetry. Skin hardness and elasticity were measured using torsional ballistometry. Ultimate tensile strength and linear stiffness were calculated using uniaxial tensile testing. Blood and oxygen flow to wounds was determined using laser doppler and supported by immunohistochemistry. Collagen deposition was investigated through use of transmission electron microscopy. The role inflammation plays in this process, as well as any molecular pathways involved, will be researched in future investigations.

Overview of mechano-modulation of burn wound repair

Fig 2.1 Overview of mechano-modulation of burn wound repair. The diagram explains the goals and approaches used in the study as well as those of future studies on mechano-modulation of burn wound repair.

Chapter 3

Results

3.1 Burn Instrument and Compression Fabric Controls

A novel burn device attached to a controlled feedback box allowed for precise measurements of temperature (Fig 3.1.A). A temperature of 200 °C was needed for the metal block to elevate the temperature of the pig skin to 100 °C to generate a full thickness burn wound (Fig. 3.1.B). After application, eight burn wounds per pig were generated that were slightly discolored, rectangular in shape and measured 6.45 cm^2 (Fig. 3.1.C). The compression garment produced about 10 mmHg of pressure on the treatment wounds with a 0.5 mmHg decrease in pressure over twelve hours caused by the prolonged stress on the material (Fig. 3.2.A). Due to hexagonal orientation of the fibers, the fabric returned to its original state and continued to produce 10 mmHg when the garments were readjusted everyday (Fig. 3.2.B).

3.1 Wound Contraction and Skin Biomechanics

Burns generated full thickness wounds which were largely re-epithelialized by day 28 (Fig. 3.3.A). Ten percent compression on treatment wounds by F47 compression fabric resulted in contraction to an average of 85 ± 5.70% of original wound area, compared to 65 ± 5.31% contraction of control wounds (Fig. 3.3.B). Skin elasticity returned to about 70% of normal pig skin and had decreased hardness with compression therapy compared to about lower elasticity and increased hardness without compression (Fig. 3.3.C). Ultimate tensile strength for treatment wounds was measured to be 2.3 MPa

compared to 1.7 MPa for the control wounds (Fig. 3.3.D). Linear stiffness for treatment wounds of 14.0 N/mm was greater than that of control wounds at 11.9 N/mm (Fig. 3.3.E).

3.2 Wound Perfusion

Laser Doppler imaging and analysis revealed no statistical difference of wound perfusion between wounds that received compression and those that did not (Fig. 3.4.A). Endothelial cell density measurements also showed no significant difference between the two wound types ($p > 0.05$), with treatment wounds having endothelial cell density of $38.3 \pm 0.7\%$ versus control wound density of $29.9 \pm 0.4\%$ (Fig. 3.4.B-C).

3.3 Collagen Fibril Diameter

Percent composition per wound of collagen fibril diameters showed varying results (Fig. 3.5.A-D)

Microstat controlled burn instrument and wound morphology

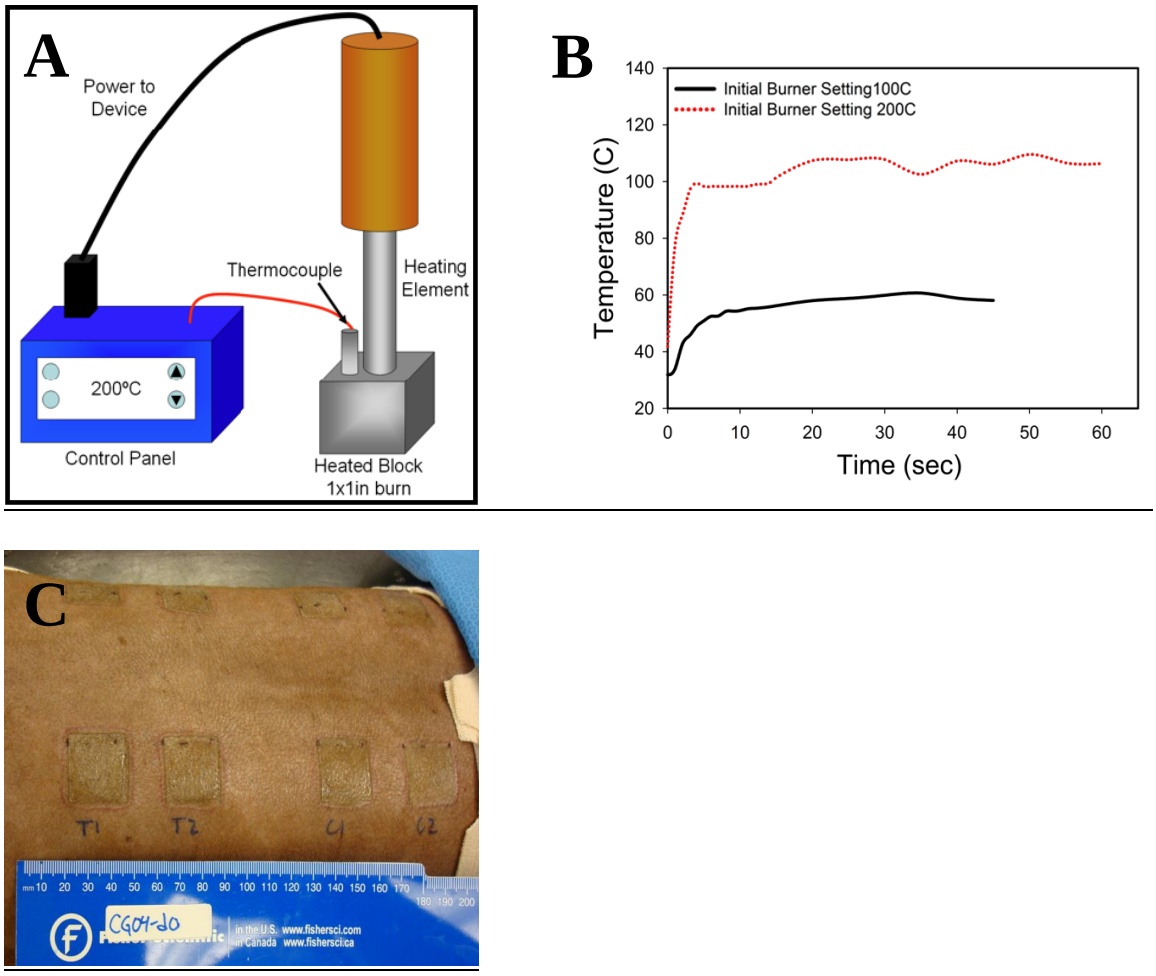

Fig 3.1 Microstat controlled burn instrument and wound morphology.(A) Schematic of the burn instrument. The metal block burner is attached to the temperature control and to the heating element. The wooden handle allows for placement of the burn instrument and the control panel allows for precise temperature measurement. (B) The initial metal block burner temperature of 100 °C elevated the porcine skin to 60 °C. The metal block burner temperature of 200 °C elevated the porcine skin to the 100 °C required to generate a full thickness burn wound. (C) The generated burn wounds are discolored and rectangular in shape.

Compression garment controls

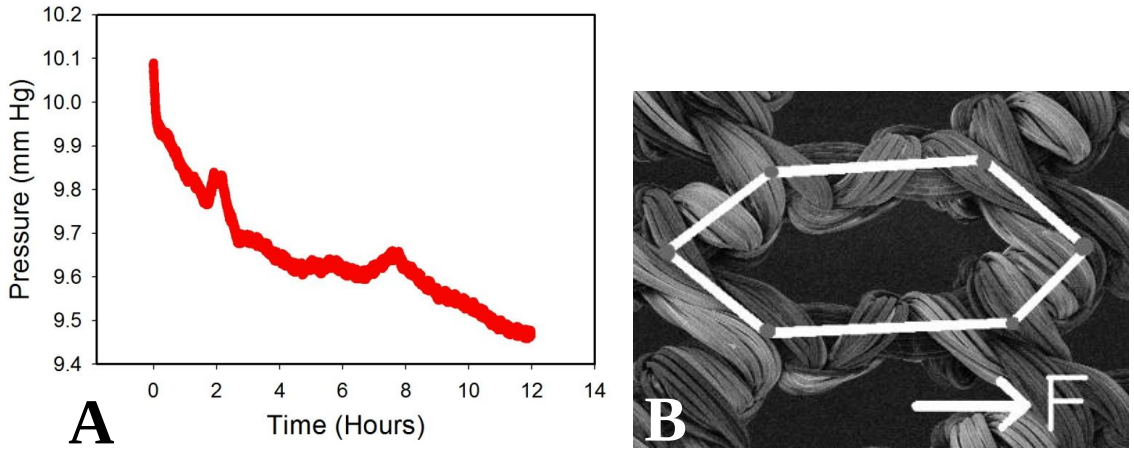

Fig 3.2 Compression fabric pressure and fiber orientation. (A) Graph of pressure versus time for 10% compression garment. Over 12 hours, the pressure decreases from about 10 mmHg to 9.5 mmHg. (B) The hexagonal orientation of the fabric fibers allows the garment to return to its original state after being stretched for prolonged periods of time.

Wound contraction and skin biomechanics

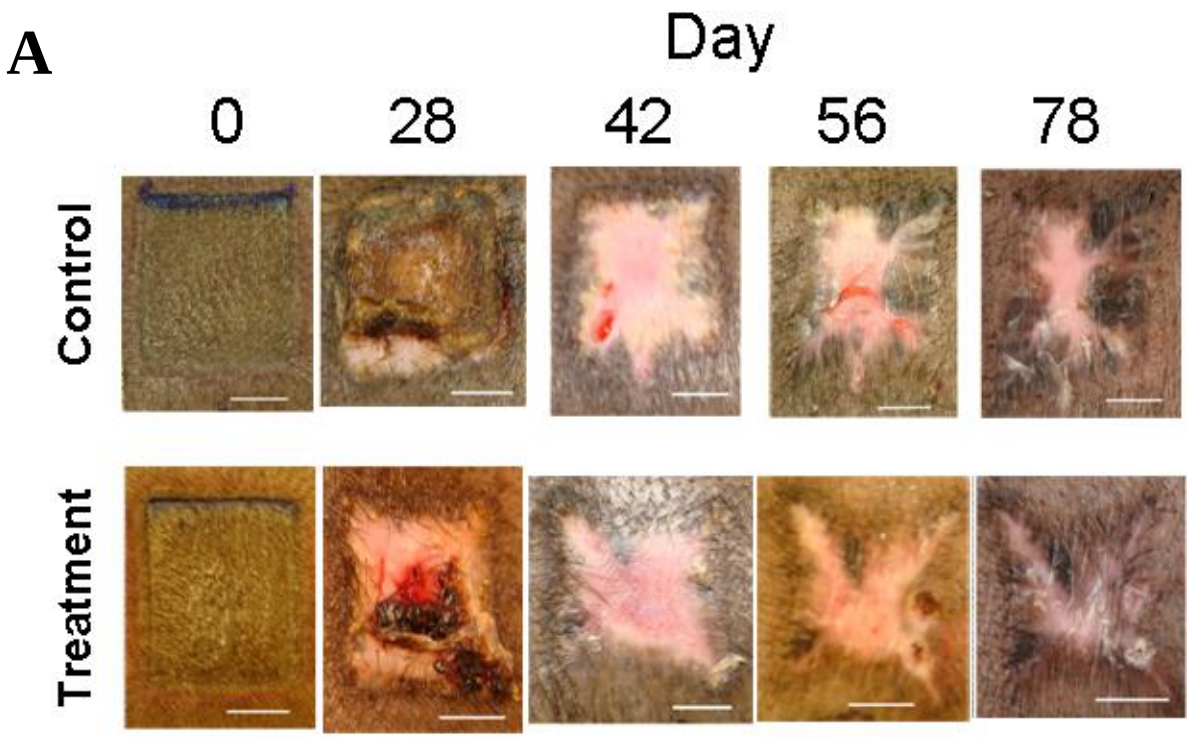

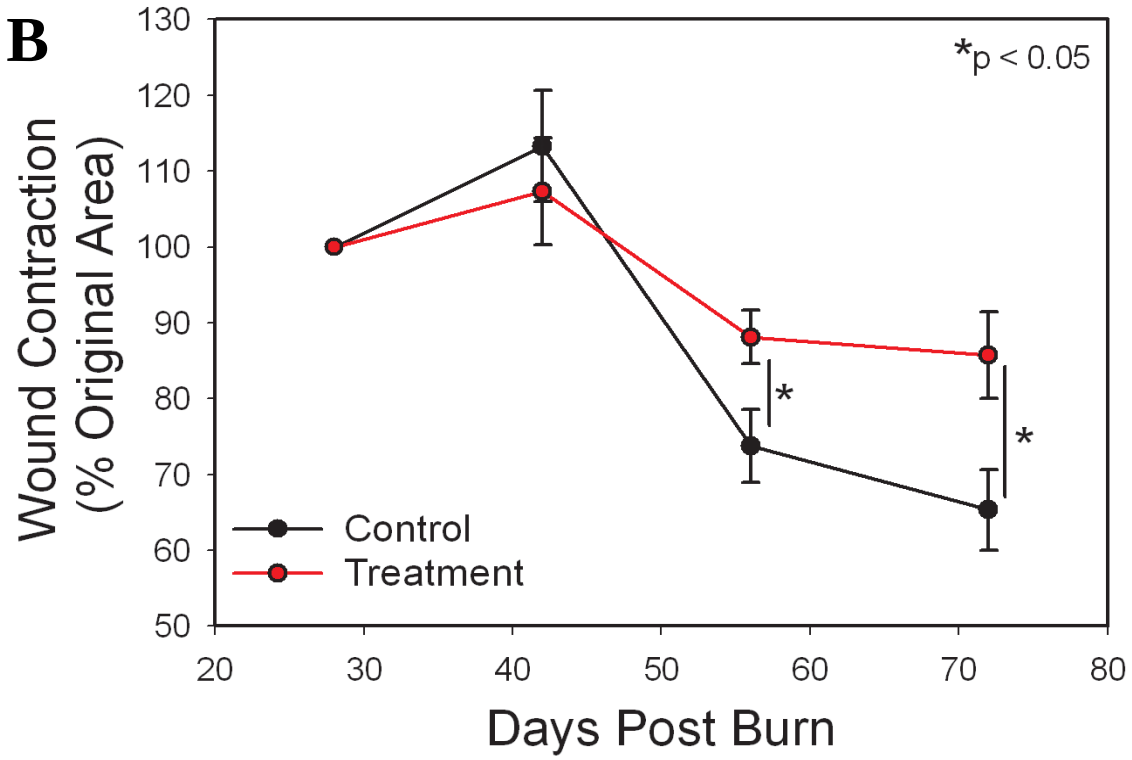

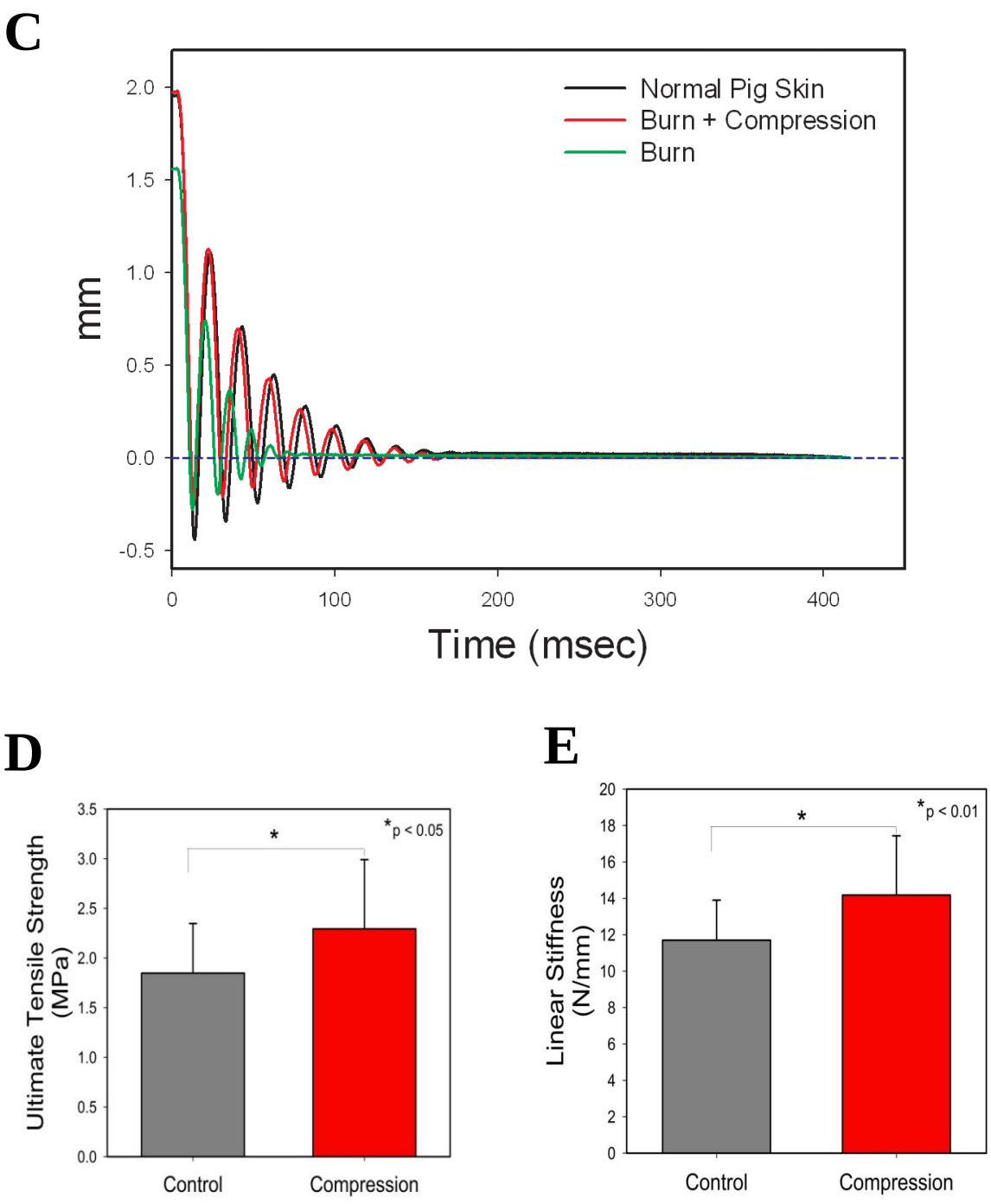

Fig 3.3 Wound contraction and skin biomechanics. (A) Burns generated full thickness wounds which were largely re-epithelialized by day 28 (scale bar = 1 cm). (B) Treatment wounds with compression contracted to 85 ± 5.70% of the original burn area, which was less than the control wounds without compression which contracted to 65 ± 5.31% of the original burn area. (C) Use of compression (red line) returned skin elasticity to 70% that

of normal pig skin (black line) and had decreased hardness. Wounds not receiving compression were less elastic (green line) and had increased hardness. (D and E) The ultimate tensile strength and linear stiffness of treatment wounds that received compression was greater (2.3 MPa, 14.0 N/mm) than that of the control wounds that didn't receive compression (1.7 MPa, 11.9 N/mm).

Wound perfusion investigated by laser doppler and endothelial cell density

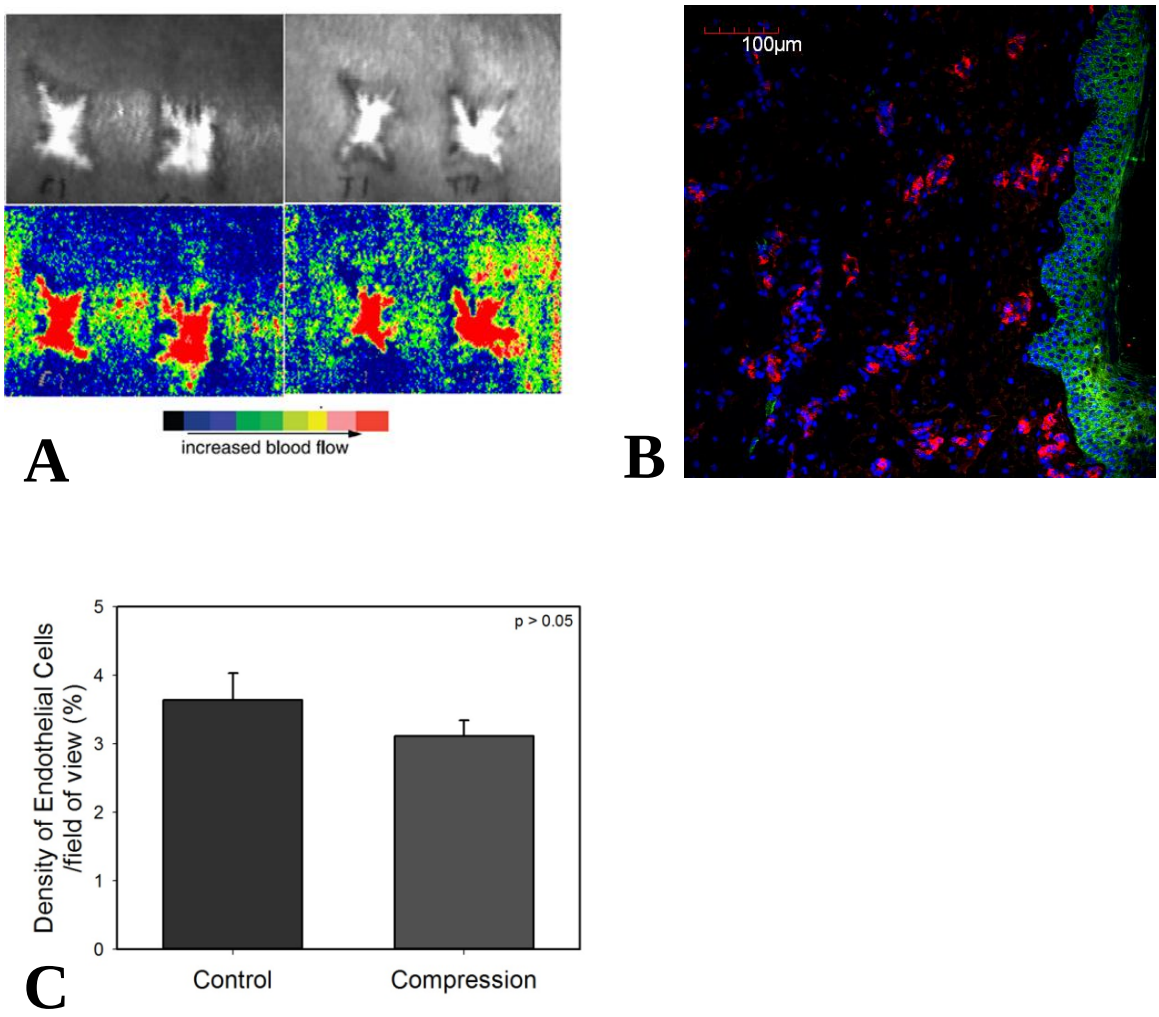

Fig 3.4 Wound perfusion analysis. (A) Laser doppler imaging of treatment and control burn wounds. Images show no difference of blood and oxygen between treatment or control wounds. (B) Von Willebrund Factor (VWF, red) stains for endothelial cells in blood vessels. DAPI (blue) stains nuclear material and basic cytokeratin (green) stains epidermis. (C) VWF staining and endothelial cell density analysis showed no difference in blood vessel content between treatment and control burn wounds.

Collagen fibril diameter and percent composition per wound

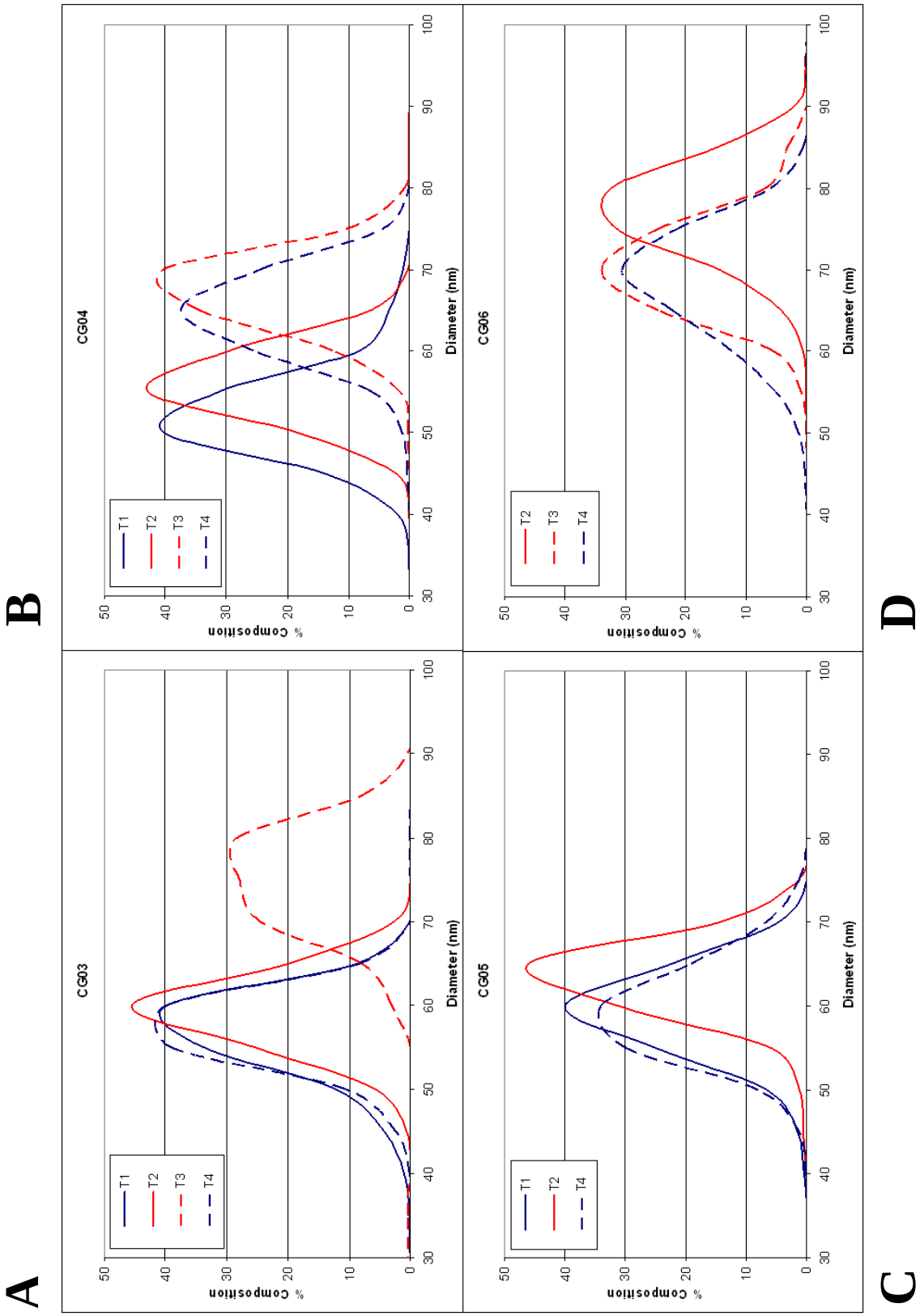

Fig 3.5 Collagen fibril diameter and percent composition per wound. Graphs are separated per pig and show percent composition of collagen fiber diameters per wound type. (A) CG03 shows both control (T1 and T4) and one treatment (T2) wound having similar fiber diameter distributions with one control (T3) with a larger average diameter. (B) CG04 shows T1 and T2 having similar distributions and T3 and T4 having similar distributions. (C) CG05 shows all sampled wounds (T1, T2 and T4) having similar distributions. (D) CG06 shows T3 and T4 having similar distributions and T2 having slightly larger fiber diameter on average.

Chapter 4

Discussion

To investigate the efficacy of compression therapy in burn wound repair, wound contraction and skin biomechanics were investigated. All burn wounds were largely re-epithelialized by day 28, but the treatment wounds with compression fabric showed far less contraction than the control wounds (Fig. 3.3.B). Contraction results in excess tension on the perimeter skin and hard scar tissue build-up in the wound bed. By preventing contraction, compression therapy was able to positively affect wound repair which was made obvious at the macroscopic level (Fig. 3.3.A). Compression therapy made burn wound skin more similar to normal porcine skin by decreasing skin hardness and increasing its elasticity, ultimate tensile strength and linear stiffness. The improvement in skin biomechanics made from compression is obvious, but the molecular events responsible remain a mystery up to this point.

Having discovered no difference in blood and oxygen flow to the wounds from the laser doppler data, and having this supported by the lack of difference in endothelial cell densities of red blood vessels in each wound type, it can be suggested that blood and oxygen flow are not responsible for the observed improvements in the treatment wound skin biomechanics. The collagen fibril diameters data is too variable to draw any solid conclusions from. In addition to this study being a variable animal model, one possible explanation for this lack of consensus is that this particular study was shorter than the standard time of six months required for full scar maturation. If an additional experiment was conducted that lasted the entire six months, we might expect to see a greater difference between the collagen fibril diameters of treatment and control wounds. If this

were the case, it might suggest that compression therapy causes a difference in collagen fibril deposition by up or down regulating a molecular pathway crucial to collagen synthesis.

In order to identify the molecular events responsible, two more aspects of wound repair will be researched. First, the role inflammation plays in this process will be investigated by quantifying macrophage density in wounds per time point. However, inflammation is thought not to be responsible for the observed biomechanical differences because inflammatory responses normally finish within 14 days, which is 14 days sooner than the application of the compression garments. Since inflammation had already come and gone by the time compression was applied, it can be treated as a common variable between the treatment and control wounds and could not be responsible for the observed biomechanical differences between the wounds.

The observed results might possibly be caused by differences in collagen gene expression. Collagen I (ColI) and Collagen III (ColIII) expression levels will be investigated using molecular techniques such as PCR and miRNA analysis to determine what role these gene pathways play in affecting scar tissue formation. The observed differences might also result from the fibroblast to myofibroblast differentiation pathway being up or down regulated. The role of compression on this pathway will also be investigated. Once the molecular pathway is found, new mechanically based therapies can be developed that reduce the required pressure applications to one or two per day and increase patient compliance. Also, non-mechanically based solutions, such as pharmaceuticals, can begin to be developed that control wound repair by up or down regulating the collagen or fibroblast differentiation pathways.

Chapter 5

Materials and Methods

5.1 Porcine Animal Model

Six female Red Duroc pigs were used as a porcine animal model for this burn wound experiment. Red Durocs are a good model system due to their easy attainability, maintenance and similarity to humans regarding skin biomechanics and burn wound studies.

5.2 Generation of Burn Wounds

Eight full-thickness, 2.5 x 2.5 cm burn wounds were generated paramedially down both the thoracic and lumbar regions (Fig. 3.1.C) using a custom designed microstat-controlled heat delivery apparatus. The device (Fig. 3.1.A) was composed of a 1 in^3 metal block heated to 200 ± 5 °C and attached to a secure wooden handle. The metal block was placed perpendicularly on the porcine skin and held for thirty seconds to generate the full-thickness burn wound.

5.3 Compression Garments and generation of compressive force

The top group of four wounds was designated the treatment group, and the bottom group of four wounds the control group (Fig. 5.1.B). The treatment wounds were wrapped in F47 compression fabric (The Marena Group Inc., Lawrenceville, GA) at a ten percent decrease in circumference compared to the circumference of the pig. This compression generated 10 mm Hg of pressure on the wounds. The control group

received no compression (Fig. 5.1.A). The compression garments were applied on day 28 at which time the wounds were dry and largely re-erpithelialized (Fig. 5.1.B top right). To obtain 10% compression, the porcine circumference was measured and 10% of the linear distance was subtracted from the circumference length. The compression garment was then wrapped around the porcine at this new circumference (Fig. 5.1.C). As the compression garment would not stay positioned on the top two wounds of the treatment group, they were treated as control wounds and replaced the old control group of the bottom four wounds. The bottom two wounds of the old treatment group stayed the treatment group and were compared to the new control group. The garments were checked and readjusted daily to allow for the natural growth of the pigs and to ensure 10% compression for the duration of the study.

5.4 Blood, Biopsies, and Ballistometry (oh my!)

Punch biopsies (4 mm) and various experimental measurements were taken on days 0, 28, 42, 56, and 78. Punch biopsies were either flash frozen in liquid nitrogen or placed into freezing medium to create blocks. They were at -80 °C for future use in immunohistochemistry. Wound contraction measurements were obtained by placing a scale ruler (scale= 1cm) next to each wound at the mentioned time points and then taking a picture. The pictures were edited using Adobe Photoshop Editor and then analyzed by computerized planimetry using imageJ software (National Institute of Health, Bethesda, MD). The wound areas from each time point were found and compared to original wound size.

Torsional ballistometry was used to measure skin elasticity and hardness for normal skin, treatment, and control wounds at each time point. The torsional ballistometer (Diastron Inc., Broomall, PA) uses a ruby tipped stylus fixed to a rigid low mass arm which is suspended at its balance point. A solenoid acts to elevate the probe tip from the test surface. Upon release, the stylus impacts the surface and oscillates around its balance position until it comes to rest. The slope of the oscillation is directly related to the elasticity of the tissue while it initial indentation is proportional to the hardness of the tissue. The graphs were collected and analyzed in SigmaPlot (Systat Software Inc., San Jose, CA) to produce a comparison graph between control, treatment, and normal pig skin.

To measure wound perfusion, blood and oxygen flow to each wound, a laser dopplar (MANUFACTURER) used at each time point. The machine was rolled over the pigs and scanned the burn wounds. As a result, computer generated pictures were produced which showed amounts of blood and oxygen flow to the wounds based on a colored scale bar.

5.5 Staining and Microscopy

Standard immunohistochemistry was used to stain tissue sections for endothelial blood vessel cells. The primaries used were Von Willebrund factor (Abcam Inc., Cambridge, MA) at 1:50 dilution and basic cytokeratin (Santa Cruz Biotechnology Inc., Santa Cruz, CA) at 1:50 dilution. The secondaries used were DAPI nucleic acid stain (Invitrogen, Eugene, OR) at 1:50 dilution, Alexa Fluor 488 donkey-anti mouse IgG (Invitrogen, Eugene, OR) and Alexa Fluor 594 donkey-anti rabbit IgG (Invitrogen,

Eugene, OR) at 1:250 dilutions each. An Olympus Fluoview FV100 Spectral Confocal microscope (Olympus, Center Valley, PA) was used to collect the images which were then processed with FV10-ASW 2.0 software (Olympus, Center Valley, PA) and Adobe Photoshop Elements 6.0 (Adobe Systems Inc., San Jose, CA). The images were cropped to ensure equal areas (250 μm x 450 μm) and then analyzed by imageJ (National Institute of Health, Bethesda, MD) for endothelial cell density.

Tissue sections were sent to Ohio State University's Campus Microscopy and Imaging Facility (CMIF) for transmission electron microscopy (TEM) preparation and viewing. TEM was used to collect cross sectional images of collagen fibrils at 68,000 times magnification. Collagen fibril images were traced onto transparency film, scanned into a computer and then analyzed using imageJ (National Institute of Health, Bethesda, MD).

5.6 Uniaxial Tensile Testing

To assess the strength of the healing wounds, skin biopsies (20 mm X 60 mm) were excised from the wound beds of the porcine 78 days post wounding (Fig. 5.2.A). Each rectangular-shaped skin biopsy was then cut into dogbone-shaped specimens (gauge length of 2 mm and gauge width of 4mm) for tensile testing. The punch was placed on the skin biopsy such that the wound was in the center of the gauge length and width (Fig. 5.2.B). The muscle fascia was then removed from each dogbone specimen using a scalpel and the thickness was measured using digital calipers. As the stress is concentrated within the gauge length of the dogbone and the wound is the weakest portion of the sample, maximum load that can be applied to the sample is a direct

function of the strength of the wound. Each specimen was then mounted into the grips of a TestResources mechanical tester model 1000R12 (Shakopee, MN) with a 50 lbf load cell (Figure 5.2.C). Load is continuously recorded as the pig skin is strained by using MTestWr Version 1.3.6 (TestResources, Shakopee, MN). Samples were strained until failure. Ultimate tensile strength was calculated by dividing the maximum load by the thickness of the sample. Linear stiffness was found by calculating the slope of the graph until failure. Results were averaged to compare treatment versus control wounds.

Compression garments and generation of compressive force

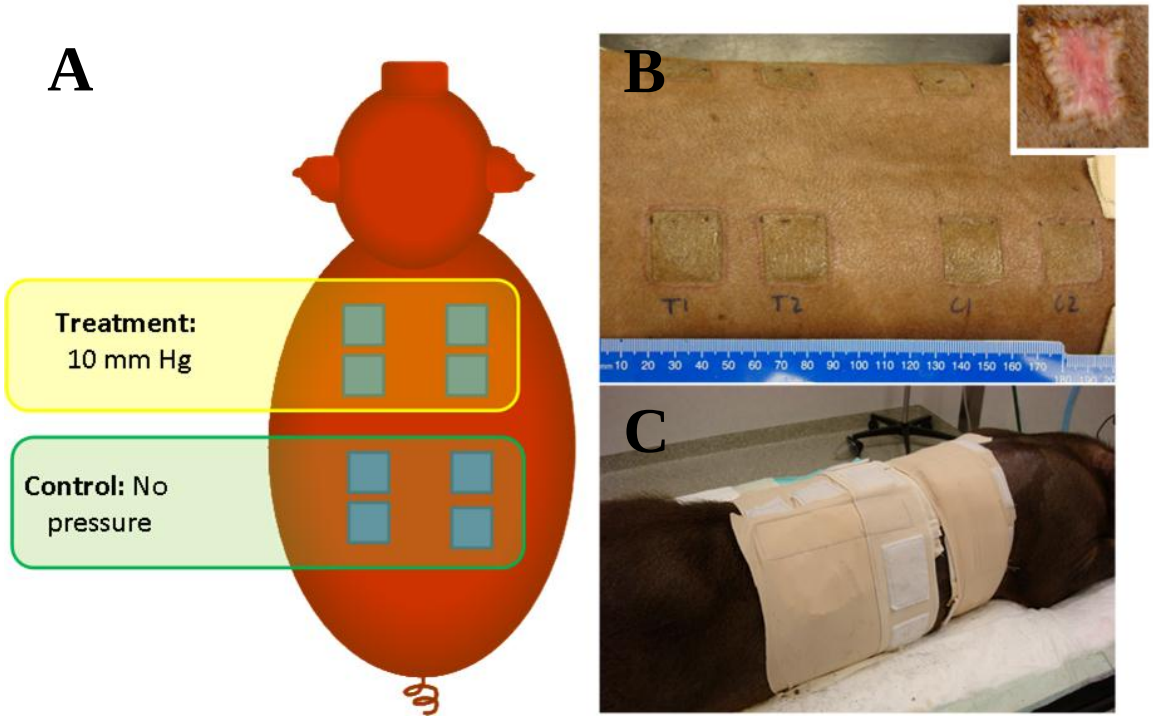

Fig 5.1 Compression garments and generation of compressive force. (A and B) The top four burn wounds served as treatment wounds and had 10% compression, or 10 mm Hg of pressure, applied to them. The bottom four wounds served as control and had no compression applied to them. (B) Red Duroc porcine with burn wounds. (B top right) Wound was re-epithelialized by day 28 to allow for application of compression garment. (C) Application of compression garment at 10% compression.

Uniaxial tensile testing of porcine skin to investigate skin biomechanics

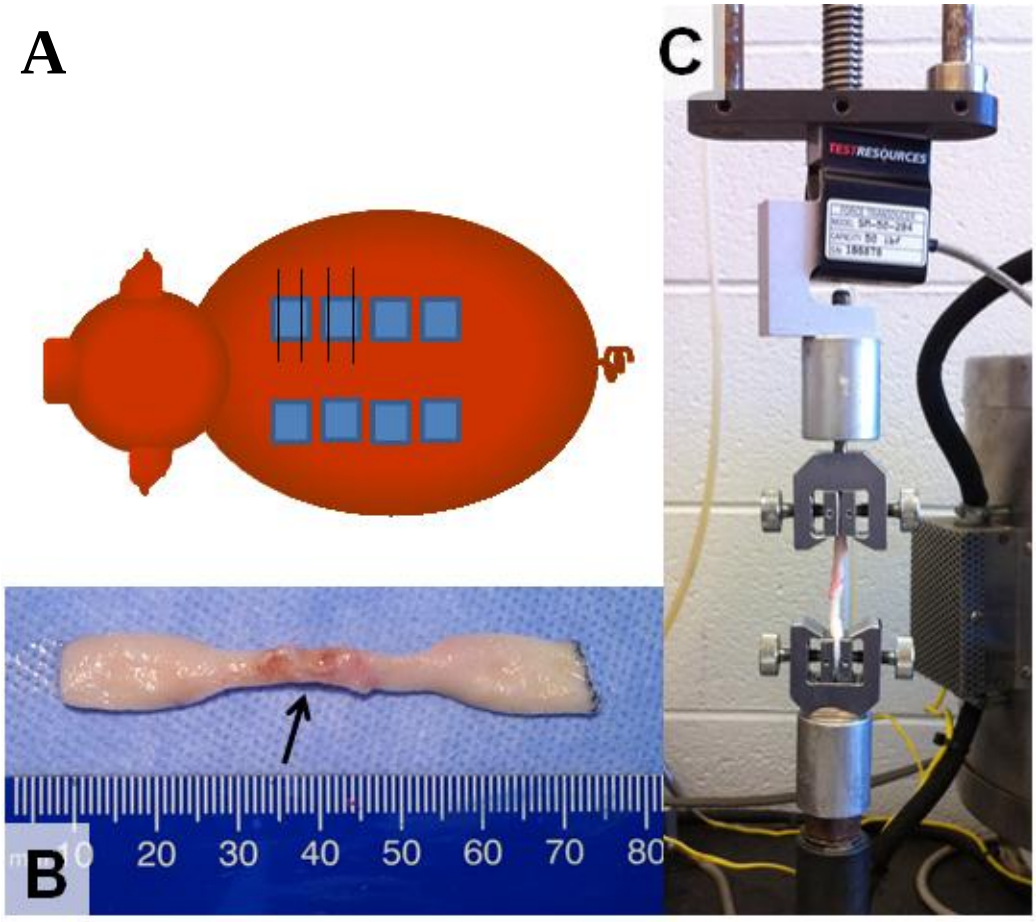

Fig 5.2 Uniaxial tensile testing of skin to investigate skin biomechanics. (A) Tissue sections (20 mm X 60 mm) were excised from the wound beds and wound perimeters of the porcine 78 days post wounding. (B) Each rectangular-shaped skin biopsy was then cut into dogbone-shaped specimens (gauge length of 2 mm and gauge width of 4mm) for tensile testing. (C) Each specimen was mounted into the grips of a TestResources mechanical tester and strained until failure.

Works Cited

1. Bock, O, Schmid-Ott, G, Malewski, P, Mrowietz, U. Quality of life of patients with keloid and hypertrophic scarring. Archives of Dermatologic Research 2006;297(10):433-438.

2. Mazharinia, N, Aghaei, S, Shayan, Z. Dermatology Life Quality Index (DLQI) scores in burn victims after revival. Journal of Burn Care Research 2007;28(2):312-317.

3. Macintyre, L, Baird, M. Pressure garments for use in the treatment of hypertrophic scars - a review of the problems associated with their use. Burns 2006;32(1):10-15.

4. Van den Kerckhove, E, Stappaerts, K, Fieuws, S, Laperre J, Massage P, Flour M, Boeck, W. The assessment of erythema and thickness on burn related scars during pressure garment therapy as a preventive measure for hypertrophic scarring. Burns 2005;31(6):696-702.

5. Fournier, R, Pierard, GE. Skin tensile strength modulation by compressive garments in burn patients. A pilot study. Journal of Medical Engineering and Technology 2000;24(6):277-280.

6. Staley, MJ, Richard, RL. Use of pressure to treat hypertrophic burn scars. Advances in Wound Care 1997;10(3):44-46.

7. Garciavelasco, M, Ley, R, Mutch, D, Surkes, N, Williams, HB. Compression treatment of hypertrophic scars in burned children. Canadian Journal of Surgery 1978;21(5):450-452.

8. Larson, DL, Abston, S, Willis, B, Linares, H, Dobrkovsky, M, Evans, EB, Lewis, SR. Contracture and scar formation in the burn patient. Clinics in Plastic Surgery 1974;1(4):653-656.

9. Kischer, C, Bunce, H, Shetlar, M. Mast cell analyses in hypertrophic scars, hypertrophic scars treated with pressure and mature scars. Journal of Investigative Dermatology 1978;70:355-357.

10. Puzey, G. The use of pressure garments on hypertrophic scars. Journal of Tissue Viability2002;12(1):11-15.

11. Giele, H, Liddiard, K, Currie, K, Wood, F. Direct measurement of cutaneous pressures generated by pressure garments. Burns 1997;19(1)17-21.

12. Mann, R, Yeong, EK, Moore, M, Colescott, D, Engrav, LH. Do custom-fitted pressure garments provide adequate pressure? Journal of Burn Care and Rehabilitation 1997;18(3):247-249.

13. Reid, WH, Evans, JH, Naismith, RS, Tully, AE, Sherwin, S. Hypertrophic scarring and pressure therapy. Burns 1987;13:S29-32.

14. Collins, J. Pressure techniques for the prevention of hypertrophic scar. Clinics in Plastic Surgery 1992;19(3):733-743.

15. Williams F, Knapp, D, Wallen, M. Comparison of the characteristics and features of pressure garments used in the management of burn scars. Burns 1998;24(4):329-335.

16. Kloti J, Ponchon, J. Conservative treatment using compression suits for second and third degree burns in children. Burns 1982;8:180-187.

17. Kischer, W, Shetlar, M, Shetlar, C. Alteration of hypertrophic scars induced by mechanical pressure. Archives of Dermatology 1975;111:60-64.

18. Baur, P, Larson, D, Stacey, T, Barratt, G Dobrkovsky, M. Ultrastructural analysis of pressure treated human hypertrophic scars. Journal of Trauma 1976;16(12):958-967.

19. Giele, H, Liddiard, K, Booth, K, Wood, F. Anatomical variations in pressures generated by pressure garments Plastic and Reconstructive Surgery 1998;101(2):247-249.

20. Isherwood, P, Robertson, J, Rossi, A. Pressure measurements beneath below-knee amputation stump bandages. British Journal of Surgery 1975;62:982-986.

21. Stewart, R, Bhagwanjee, AM, Mbakaza, Y, Binase, T. Pressure garment adherence in adult patients with burn injuries, an analysis of patient and clinical perceptions. American Journal of Occupational Therapy 2000;54(6):598-606.

22. Johnson, J, Greenspan, B, Gorga, D, Nagler, W, Goodwin, C. Compliance with pressure garment use in burn rehabilitation. Journal of Burn Care and Rehabilitation 1995;15(2):180-188.

23. Rose, M, Deitch, E. The effective use of a tubular compression bandage, tubigrip, for burn scar therapy in a growing child. Journal of Burn Care and Rehabilitation 1983;4:197-201.

24. Kealey, G, Jensen, K, Laubenthal, K, Lewis, R. Prospective randomized comparison of two types of pressure therapy garments. Journal of Burn Care and Rehabilitation 1990;11(4):334-336.

25. Sullivan, TP, Eaglstein, WH, Davis, SC, Mertz, P. The pig as a model for human wound healing. Wound repair and regeneration 2001;9:66-76.